Title

Determinants of second-order bile duct visualization at CT cholangiography in potential living liver donors.

Journal

American Journal of Roentgenology, 200(5)

ISSN

0361-803X

Authors

Keedy, Alexander W

Breiman, Richard S

Webb, Emily M

et al.

Publication Date

2013-05-01

DOI

10.2214/ajr.11.8364

Peer reviewed

HHS Public Access

Author manuscript

AJR Am J Roentgenol. Author manuscript; available in PMC 2017 February 14.

Published in final edited form as:

AJR Am J Roentgenol. 2013 May ; 200(5): 1028–1033. doi:10.2214/AJR.11.8364.

Determinants of Second-Order Bile Duct Visualization at CT Cholangiography in Potential Living Liver Donors

Alexander W. Keedy[1], **Richard S. Breiman**[1], **Emily M. Webb**[1], **John P. Roberts**[2], **Fergus V. Coakley**[1], and **Benjamin M. Yeh**[1]

[1]Department of Radiology and Biomedical Imaging, Abdominal Imaging Section, University of California, San Francisco, 505 Parnassus Ave, M-372, San Francisco, CA 94143-0628.

[2]Department of Surgery, Division of Transplantation, University of California, San Francisco, San Francisco, CA.

Abstract

OBJECTIVE—The purpose of this article is to investigate the determinants of second-order bile duct visualization at CT cholangiography in living potential liver donors.

MATERIALS AND Methods—We retrospectively identified 143 potential living liver donors (83 men and 60 women; mean age, 37 years) evaluated with CT cholangiography, which included a slow infusion of iodipamide meglumine with CT acquisition 15 minutes after biliary contrast agent administration. Two readers independently scored the visualization of the second-order bile duct branches on a previously established 4-point scale (0 = not seen, 1 = faintly seen, 2 = well seen, and 3 = excellent visualization). Multivariate analysis was used to investigate the correlation between visualization scores and potential determinants of second-order bile duct opacification, specifically age, body mass index, creatinine level, total and direct bilirubin levels, alkaline phosphatase level, aspartate aminotransferase level, alanine aminotransferase level, patient maximum linear width, CT noise, and hepatosplenic attenuation difference at unenhanced CT.

RESULTS—The mean (± SD) second-order bile duct visualization scores were 2.35 ± 0.66 and 2.55 ± 0.60 for readers 1 and 2, respectively. In the multivariate analysis, the only independent predictors of reduced second-order bile duct visualization were higher alkaline phosphatase level ($p = 0.01$) and higher CT noise ($p = 0.02$).

CONCLUSION—Higher serum alkaline phosphatase level and higher CT noise in potential living liver donors indicate a higher risk of poor second-order bile duct visualization at CT cholangiography.

Keywords

bile duct visualization; CT cholangiography; liver donor

Preoperative hepatobiliary imaging is arguably the most pivotal test for determining whether a potential living liver donor is physically appropriate for liver donation. In particular, preoperative determination of second-order bile duct branch anatomy plays a key role in

Address correspondence to B. M. Yeh (Benjamin.Yeh@ucsf.edu).

preoperative biliary evaluation because right-sided second-order bile duct variants occur in up to 54% of patients [1, 2] and because of the presence of biliary anatomic variants known to be associated with posttransplantation biliary complications, including graft-threatening leak and strictures. CT cholangiography has shown excellent accuracy for the preoperative evaluation of living potential liver donors [1–5] and compares favorably with MR cholangiography [4, 6, 7], endoscopic retrograde cholangiography [3, 8, 9], and intraoperative cholangiography [4, 8]. At our own institution, CT cholangiograms are obtained for all potential liver transplant donors instead of MRCP.

Although CT cholangiography has been shown to accurately depict second-order biliary branch anatomy [4, 10] and to eliminate the need for intraoperative cholangiography during hepatic lobe retrieval [1], a small portion of CT cholangiograms are suboptimal [1, 2]. The reasons for poor bile duct visulization in healthy potential liver donors are poorly understood and not well studied. In patient populations with possible biliary disease, poor bile duct visualization at CT cholangiography has been associated with abnormally high levels of serum total bilirubin [9, 11, 12], a situation that is uncommon in potential living liver donors. Knowledge of the factors that contribute to poor-quality CT cholangiograms in the potential living liver donor population is essential to optimize CT cholangiograms or to triage to an alternative protocol or imaging modality to avoid the costs, radiation, and delay associated with a non–diagnostic-quality examination. Therefore, we undertook this study to assess the ability of serologic liver biochemical tests, clinical measures, and factors related to patient body habitus to predict second-order bile duct visualization at CT cholangiography for potential living liver donors.

Materials and Methods

Subjects

This was a retrospective single-institution study approved by our Committee on Human Research. Patient informed consent was not required. Our study was compliant with the HIPAA. No industry support was provided for this study, and the authors have no conflicts of interest to disclose. We retrospectively identified 143 consecutive CT cholangiograms of living donor candidates that were obtained at our institution between January 2001 and March 2005. The study population included 83 men and 60 women with a mean age of 37 years (range, 18–56 years).

CT Cholangiography Technique

All patients underwent CT cholangiography immediately after a single unenhanced axial image was obtained through the liver and spleen to assess for liver steatosis, and CT angiography evaluation was performed of hepatic vasculature, liver volume, and liver parenchyma. At CT cholangiography, 20 mL of 52% iodipamide meglumine (Cholografin, Bracco Diagnostics) diluted in 80 mL of normal saline was infused over 30 minutes. The liver was imaged during a single breath-hold 15 minutes after completion of the biliary contrast agent infusion. In cases of suboptimal visualization at 15 minutes, a second scan was obtained at 35 minutes after completion of the biliary contrast infusion. The section thickness, gantry rotation time, tube current, tube voltage, and tabletop speed for the CT

scans were 1.25 mm, 0.8 seconds, automatic exposure control (SmartmA, GE Healthcare) with a noise index of 11.7 and maximum tube current of 440 mA, 120 kVp, and 13.5 mm/s, respectively. Standard kernel image reconstruction was used. No iterative reconstruction technique was used because it was not available. The mean total radiation dose for the examination was 7.6 mSv. Examinations were performed on MDCT scanners (LightSpeed, GE Healthcare) without oral contrast material. Before the administration of cholangiographic contrast material, each subject received 25 mg of IV diphenhydramine (Benadryl, Pfizer) because of the perceived high risk of allergic reaction with this agent. The initial subjects examined (n = 43) were also given IV morphine sulfate (LifeCare, Abbott Laboratories; 0.04 mg/kg of body weight) with the intent to contract the sphincter of Oddi [13–15] and possibly improve biliary distention. However, IV administration of morphine did not significantly improve CT cholangiographic bile duct visualization, so the remaining patients (n = 100) were not given morphine.

CT Interpretation

Two radiologists with subspecialty training in abdominal imaging independently reviewed all the CT images on a PACS workstation (Impax, Agfa). The radiologists were unaware of the serum biochemical laboratory test results and clinical data. Readers were able to use all imaging information available, which included the axial images, multiplanar reformats, maximum intensity projections, and volume-rendered reconstructions, but focused mainly on the 1.25-mm-thick source axial images. Visualization of the branches of the biliary tract was scored according to the following scale: 0, not seen; 1, faintly seen; 2, well seen except for the confluence or a portion of the biliary segment; and 3, excellent visualization of the entire branch. See Figures 1 and 2 for representative samples of biliary tract visualization scoring. Biliary branches included in this analysis were the common hepatic duct, cystic duct, first-order branches (right main hepatic duct and left main hepatic duct), second- order branches (right anterior hepatic duct, right posterior hepatic duct, left medial hepatic duct, and left lateral hepatic duct), and third-order branches (right anterior hepatic ducts, right posterior hepatic ducts, left medial hepatic ducts, and left lateral hepatic ducts). Collective visualization scores (e.g., all second-order branches) were determined by calculating the mean score for all branches of that order.

Clinical Measures

The serum alkaline phosphatase, aspartate aminotransferase, alanine aminotransferase, total bilirubin, direct bilirubin, and creatinine values before the CT cholangiography examination were recorded. The median interval between the serum tests and the CT cholangiograms was 2 days (range, 0–48 days; 125 patients, ≤ 14 days; 18 patients, ≥ 15 days). The clinical measures included age, sex, and body mass index (BMI; calculated by dividing the patient weight in kilograms by the square of the patient height in meters), which were recorded before CT cholangiography examination with a median interval of 2 days (range, 0–51 days).

Imaging Assessment of Patient Body Habitus and Noise

In addition to BMI, factors related to the patient body habitus that were evident on the CT images were assessed. The maximum linear width was the maximum transverse diameter of

the patient at the level of the porta hepatis. The CT noise was estimated by measuring the SD of the CT attenuation number (in Hounsfield units) in a 2-cm^2 region of interest containing only gas and placed 1 cm anterior to the ventral abdominal surface at the level of the liver.

Imaging Assessment of Hepatic Steatosis

Hepatic fatty infiltration was assessed at CT on a single unenhanced axial image through the liver and spleen as follows: three regions of interest at least 2 cm^2 in size were drawn in the right lobe of the liver in areas away from large blood vessels, and two similarly sized regions of interest were drawn in the spleen. The difference between the mean attenuation in the hepatic and splenic regions of interest was used as a quantitative measure of hepatic steatosis, such that more negative values indicated a greater degree of steatosis [16–19].

All patients also underwent routine liver ultrasound as part of the evaluation of potential liver donation. The median interval between the CT and ultrasound examination was 0 days (range, 0–43 days). Hepatic fatty infiltration was assessed at ultrasound by noting diffusely increased echogenicity of hepatic parenchyma, poor sonographic penetrance, and regions of focal fatty sparing [18–21]. A dichotomous assessment of the presence or absence of diffuse fatty infiltration was subjectively determined by a radiologist with subspecialty training in ultrasound.

Statistical Analysis

Statistical analysis was performed using R statistical software (version 2.5.1, The R Project). Correlation of bile duct visualization score with biochemical and clinical parameters was determined using the Pearson correlation coefficient. Interobserver agreement was assessed with weighted kappa statistics. The level of agreement was defined as follows: κ = 0–0.20, poor agreement; κ = 0.21–0.40, fair agreement; κ = 0.41–0.60, moderate agreement; κ = 0.61–0.80, good agreement; and κ = 0.81–1.00, very good agreement [22]. The parameters with a p value of less than 0.20 in the univariate analysis were included as covariates in a multivariate generalized estimating analysis with fixed effect for patient using second-order bile duct visualization as the outcome variable. This model was performed using a backward selection method as a means of decreasing the likelihood of excluding negatively confounding factors [23, 24]. For the purposes of threshold value determination, if the second-order bile duct visualization score was less than 2, it was considered reduced biliary visualization. Threshold values for alkaline phosphatase and CT noise were determined using receiver operating characteristic analysis. From the receiver operating characteristic analysis, the value that provided the maximum for the Youden index, which was calculated as index value = sensitivity – (1 – specificity), was selected as the threshold value for determining the diagnostic test characteristics [25]. A p value of less than 0.05 was considered statistically significant.

Results

Visualization Scores and Clinical Factors

The mean second-order bile duct visualization scores were 2.35 ± 0.66 and 2.55 ± 0.60 for readers 1 and 2, respectively. Twenty-three (16%) and 14 (10%) cases were classified as poorer biliary visualization for readers 1 and 2, respectively. The visualization scores for the individual second-order ducts and other bile ducts are found in Table 1. Interobserver agreement was good, with a kappa value of 0.70 for all second-order bile ducts. Two minor contrast material reactions were noted, consisting of one case of mild self-limiting urticaria and one case of mild wheezing. Neither of these reactions required treatment.

Mean values for all serum tests were within the normal range (Table 2). Serum biochemical test results were within the normal range in 734 of 767 total measurements (96%), and 114 of 143 patients (80%) had all serum test results in the normal range. There was a statistically significant negative correlation between BMI and CT hepatosplenic attenuation difference ($r = -0.23$; $p = 0.01$), with a higher BMI being associated with greater hepatic steatosis.

Predictors of Biliary Branch Visualization

Among the serum tests, only alkaline phosphatase showed a significant negative correlation with CT cholangiogram visualization scores for second-order bile ducts ($r = -0.31$ and -0.22 for readers 1 and 2, respectively; $p \leq 0.01$) (Table 3). For neither reader did serum total bilirubin, direct bilirubin, creatinine, aspartate aminotransferase, or alanine aminotransferase correlate with biliary branch visualization ($p > 0.07$ for all comparisons). BMI showed significant negative correlation with second-order bile duct visualization scores ($r = -0.28$ and -0.29 for readers 1 and 2, respectively; $p \leq 0.002$). For neither reader did patient age or sex correlate with biliary branch visualization ($p > 0.74$ for all comparisons). A statistically significant correlation was observed between second-order biliary visualization and patient maximum linear width ($r = -0.22$ and -0.21; $p \leq 0.01$ for both comparisons) and CT noise ($r = -0.32$ and -0.31; $p < 0.001$ for both comparisons) for both readers. The hepatosplenic CT attenuation difference showed a statistically significant correlation with second-order bile duct visualization scores for reader 2 ($r = 0.22$; $p = 0.01$) but did not achieve statistical significance for reader 1 ($r = 0.16$; $p = 0.06$).

In the multivariate analysis, higher alkaline phosphatase level ($p = 0.01$) and higher CT noise ($p = 0.02$) were the only variables independently associated with reduced second- order bile duct visualization. The serum alanine aminotransferase level, BMI, patient maximum linear width, and hepatosplenic CT attenuation difference did not achieve statistical significance ($p > 0.19$ for all comparisons; Table 4). The Wald chi-square statistic and p value for the entire model were 24.5 and < 0.001, respectively.

Threshold Values and Test Characteristics

A threshold value of 78 IU/L for the alkaline phosphatase level yielded a positive predictive value of 0.44 and negative predictive value of 0.76 for reduced biliary visualization. A threshold value of 17 HU for the CT noise yielded a positive predictive value of 0.31 and negative predictive value of 0.84 for reduced biliary visualization.

Discussion

Our results show that an elevated serum alkaline phosphatase level and higher CT noise are independent, albeit weak, predictors of reduced second-order bile duct visualization at CT cholangiography in potential living liver donors. These findings identify a potential population of patients for whom optimization of CT cholangiography technique may be directed and contribute to the paucity of data regarding patient factors that influence the quality of these examinations. Specifically, in our study population, a patient with an alkaline phosphatase level of greater than 78 IU/L had a 44% chance of reduced biliary visualization, and a study with CT noise of greater than 17 HU had a 31% chance of reduced biliary visualization (as compared with a chance of approximately 13% for all patients in our study) and, thus, may benefit from technique optimization.

Potential methods of CT cholangiography technique optimization include increasing the dose or duration of contrast material administration [9], the use of higher CT tube current settings and noise-reduction reconstruction algorithms, using automatic exposure control, or perhaps the use of dual-energy CT cholangiography [26]. Because the mechanisms of biliary visualization are dissimilar among the available biliary imaging modalities, it is realistic to posit that a biliary system that is suboptimally visualized by one modality may be adequately evaluated by use of a different modality. As such, referral to MRCP is an alternate method of preoperative anatomic biliary depiction. An evaluation of successful MRCP after poor biliary visualization at CT cholangiography is outside the scope of this study but represents an important area of further investigation.

It is important to note that our study focused on potential living liver donors, who typically are healthy and without significant hepatobiliary disease, because this is the primary population of patients who undergo CT cholangiography in the United States. Although prior studies show results different from ours, particularly showing that abnormally high levels of serum bilirubin are associated with decreased biliary opacification at CT cholangiography [11, 12], those studies focused on patients with suspected hepatobiliary disease rather than a relatively healthy population. Our results lend support to the notion that there is probably a threshold value for serum bilirubin below which there is no effect on the excretion of biliary contrast [11]. The healthy patients in our study largely had serum bilirubin levels below that threshold, explaining the lack of correlation between bilirubin and biliary visualization.

Our results support those of Owen et al. [27], who assessed oral cholecystograms of patients with normal bilirubin levels and found poorer gallbladder opacification in patients with higher serum alkaline phosphatase levels, but not bilirubin or aspartate aminotransferase levels. The reason why serum alkaline phosphatase, but not other serum markers of hepatobiliary health, correlated with biliary opacification in healthy subjects at CT cholangiography is not intuitive is because elevated serum alkaline phosphatase levels are not directly related to biliary obstruction but rather are associated with increased synthesis of the enzyme. Because iodipamide excretion is believed to occur via an energy-dependent carrier [28], it is possible that the process of alkaline phosphatase synthesis may compete for adenosine triphosphate or other hepatocellular processes required for adequate iodipamide

secretion, resulting in decreased opacification and visualization of the bile ducts. This explanation is speculative, because our experiment was not designed to explore this process.

The explanation for the inverse correlation of CT noise with biliary visualization is more straightforward. Given the very small caliber of the second-order bile ducts, increased image noise would be expected to have a dramatic negative impact on the ability to adequately visualize the biliary anatomy. It is noteworthy that, although BMI, patient maximum linear width, CT noise, and the CT hepatosplenic attenuation difference all correlated with biliary visualization in the univariate analysis, only increased CT noise was retained as an independent predictor of poorer biliary visualization in the multivariate analysis. In general, larger patient girth results in a greater distance that electromagnetic radiation must penetrate through tissue to reach the detector [29, 30], with resultant increases in image noise. As such, body habitus, girth, body composition and density, and tube current are all relevant to image quality; our results suggest that this multifactorial process is more directly assessed with the CT noise. This finding highlights the potential importance of automatic exposure control and noise-reduction reconstruction algorithms in CT cholangiography technique optimization.

In addition to these anatomic considerations, obese patients are known to have increased bile acid secretion and bile acid pools sizes [31], both of which may contribute to dilution of excreted contrast material and, hence, poorer visualization at CT. The inverse correlation of BMI with biliary visualization has been previously found [32]. This finding is notable because, although the iodipamide meglumine package insert recommends a dose of 20 mL per patient (Cholografin package insert, Bracco Diagnostics), there is a theoretic benefit to adjusting the dose on the basis of patient size.

Our anecdotal observations have suggested a possible relationship between diffuse fatty infiltration and poorer biliary visualization at CT cholangiography. The results from our study suggest that such a correlation is likely present, because we observed worse biliary visualization with increasing hepatosplenic attenuation difference, the CT marker of hepatic steatosis. However, in the multivariate analysis, hepatic steatosis was not retained as independent predictor of biliary visualization, presumably related to the interaction between higher BMI and degree of fatty infiltration in the liver. It is interesting that no correlation was observed between the sonographic assessment of hepatic steatosis and biliary visualization, despite reports in the literature of similar diagnostic accuracy of CT and ultrasound for hepatic steatosis [33, 34]. The most likely explanation relates to the dichotomous nature of the ultrasound determination of steatosis, which decreases the statistical power of this test, compared with CT, which gives a continuous range of values for the extent of steatosis [35, 36].

There are several limitations to our study. The correlations observed in our study were weak and cannot reliably predict which patients will have poor biliary visualization at CT cholangiography. However, these measures do identify a group of patients at higher risk of poor biliary visualization who may benefit from CT technique optimization; thus, the low predictive values are still potentially useful. In addition, for a minority of patients, there was a long interval between the biochemical tests and the CT cholangiogram. However, the

median interval was short (2 days), and excluding the patients with an interval of greater than 30 days did not change the statistical significance of any of the results, so these patients remained in the study population.

In conclusion, though standard serologic hepatobiliary biochemical tests and image noise do not reliably predict which potential living liver donors will have poor-quality CT cholangiograms, they do offer a means to identify a subpopulation of patients at risk for poorer bile duct visualization at CT cholangiography who may benefit from technique optimization. In particular, high serum alkaline phosphatase level and higher CT image noise correlated negatively with bile duct visualization and may be more sensitive predictors of poor CT cholangiography examinations than serum bilirubin level in the potential living liver donor population. Further study of modified CT cholangiogram technique in this at-risk population is warranted.

References

1. Wang ZJ, Yeh BM, Roberts JP, Breiman RS, Qayyum A, Coakley FV. Living donor candidates for right hepatic lobe transplantation: evaluation at CT cholangiography—initial experience. Radiology. 2005; 235:899–904. [PubMed: 15833987]
2. Schroeder T, Radtke A, Kuehl H, Debatin JF, Malago M, Ruehm SG. Evaluation of living liver donors with an all-inclusive 3D multi-detector row CT protocol. Radiology. 2006; 238:900–910. [PubMed: 16439567]
3. Cheng YF, Lee TY, Chen CL, Huang TL, Chen YS, Lui CC. Three-dimensional helical computed tomographic cholangiography: application to living related hepatic transplantation. Clin Transplant. 1997; 11:209–213. [PubMed: 9193844]
4. Yeh BM, Breiman RS, Taouli B, Qayyum A, Roberts JP, Coakley FV. Biliary tract depiction in living potential liver donors: comparison of conventional MR, mangafodipir trisodium-enhanced excretory MR, and multi-detector row CT cholangiography—initial experience. Radiology. 2004; 230:645–651. [PubMed: 14990830]
5. Radtke A, Nadalin S, Sotiropoulos GC, et al. Computer-assisted operative planning in adult living donor liver transplantation: a new way to resolve the dilemma of the middle hepatic vein. World J Surg. 2007; 31:175–185. [PubMed: 17180479]
6. Schroeder T, Malago M, Debatin JF, Goyen M, Nadalin S, Ruehm SG. “All-in-one” imaging protocols for the evaluation of potential living liver donors: comparison of magnetic resonance imaging and multidetector computed tomography. Liver Transpl. 2005; 11:776–787. [PubMed: 15973711]
7. McSweeney SE, Kim TK, Jang HJ, Khalili K. Biliary anatomy in potential right hepatic lobe living donor liver transplantation (LDLT): the utility of CT cholangiography in the setting of inconclusive MRCP. Eur J Radiol. 2012; 81:6–12. [PubMed: 21041052]
8. Dorenbusch MJ, Maglinte DD, Micon LT, Graffis RA, Turner WW Jr. Intravenous cholangiography and the management of choledocholithiasis prior to laparoscopic cholecystectomy. Surg Laparosc Endosc. 1995; 5:188–192. [PubMed: 7633644]
9. Stockberger SM, Wass JL, Sherman S, Lehman GA, Kopecky KK. Intravenous cholangiography with helical CT: comparison with endoscopic retrograde cholangiography. Radiology. 1994; 192:675–680. [PubMed: 8058932]
10. Toyoda H, Hayakawa K, Kikkawa M, et al. Usefulness of three-dimensional CT cholangiography for patients prior to laparoscopic cholecystectomy. Radiat Med. 2000; 18:161–166. [PubMed: 10972546]
11. Alibrahim E, Gibson RN, Vincent J, Speer T, Collier N, Jardine C. Spiral computed tomographyintravenous cholangiography with three-dimensional reconstructions for imaging the biliary tree. Australas Radiol. 2006; 50:136–142. [PubMed: 16635032]

12. Cabada Giadás T, Sarría Octavio de Toledo L, Martínez-Berganza Asensio MT, et al. Helical CT cholangiography in the evaluation of the biliary tract: application to the diagnosis of choledocholithiasis. Abdom Imaging. 2002; 27:61–70. [PubMed: 11740611]
13. Flancbaum L, Alden SM. Morphine cholescintigraphy. Surg Gynecol Obstet. 1990; 171:227–232. [PubMed: 2385816]
14. Flancbaum L, Alden SM, Trooskin SZ. Use of cholescintigraphy with morphine in critically ill patients with suspected cholecystitis. Surgery. 1989; 106:668–673. discussion, 673–674. [PubMed: 2799641]
15. Helm JF, Venu RP, Geenen JE, et al. Effects of morphine on the human sphincter of Oddi. Gut. 1988; 29:1402–1407. [PubMed: 3197985]
16. Piekarski J, Goldberg HI, Royal SA, Axel L, Moss AA. Difference between liver and spleen CT numbers in the normal adult: its usefulness in predicting the presence of diffuse liver disease. Radiology. 1980; 137:727–729. [PubMed: 6934563]
17. Kodama Y, Ng CS, Wu TT, et al. Comparison of CT methods for determining the fat content of the liver. AJR. 2007; 188:1307–1312. [PubMed: 17449775]
18. Ricci C, Longo R, Gioulis E, et al. Noninvasive in vivo quantitative assessment of fat content in human liver. J Hepatol. 1997; 27:108–113. [PubMed: 9252082]
19. Roldan-Valadez E, Favila R, Martinez-Lopez M, Uribe M, Mendez-Sanchez N. Imaging techniques for assessing hepatic fat content in nonalcoholic fatty liver disease. Ann Hepatol. 2008; 7:212–220. [PubMed: 18753987]
20. Palmentieri B, de Sio I, La Mura V, et al. The role of bright liver echo pattern on ultrasound B-mode examination in the diagnosis of liver steatosis. Dig Liver Dis. 2006; 38:485–489. [PubMed: 16716779]
21. Saverymuttu SH, Joseph AE, Maxwell JD. Ultrasound scanning in the detection of hepatic fibrosis and steatosis. Br Med J (Clin Res Ed). 1986; 292:13–15.
22. Landis JR, Koch GG. The measurement of observer agreement for categorical data. Biometrics. 1977; 33:159–174. [PubMed: 843571]
23. Allen, DM., Cady, FB. Analyzing experimental data by regression. Belmont, CA: Lifetime Learning Publications; 1982. p. 394
24. Sun GW, Shook TL, Kay GL. Inappropriate use of bivariable analysis to screen risk factors for use in multivariable analysis. J Clin Epidemiol. 1996; 49:907–916. [PubMed: 8699212]
25. Perkins NJ, Schisterman EF. The inconsistency of “optimal” cutpoints obtained using two criteria based on the receiver operating characteristic curve. Am J Epidemiol. 2006; 163:670–675. [PubMed: 16410346]
26. Sommer CM, Schwarzwaelder CB, Stiller W, et al. Dual-energy computed-tomography cholangiography in potential donors for living-related liver transplantation: initial experience. Invest Radiol. 2010; 45:406–412. [PubMed: 20458249]
27. Owen JP, Keir MJ, Lavelle MI, Smith PA. Alkaline phosphatase and the oral cholecystogram. Br J Radiol. 1980; 53:605–606. [PubMed: 6448646]
28. Rosati G, Schiantarelli P. Biliary excretion of contrast media. Invest Radiol. 1970; 5:232–243. [PubMed: 5509451]
29. Coppenrath E, Schmid C, Brandl R, Szeimies U, Hahn K. Spiral CT of the abdomen: weight-adjusted dose reduction (in German). Rofo. 2001; 173:52–56. [PubMed: 11225418]
30. Aldrich JE, Chang SD, Bilawich AM, Mayo JR. Radiation dose in abdominal computed tomography: the role of patient size and the selection of tube current. Can Assoc Radiol J. 2006; 57:152–158. [PubMed: 16881472]
31. Bennion LJ, Grundy SM. Effects of obesity and caloric intake on biliary lipid metabolism in man. J Clin Invest. 1975; 56:996–1011. [PubMed: 1159099]
32. Schindera ST, Nelson RC, Paulson EK, DeLong DM, Merkle EM. Assessment of the optimal temporal window for intravenous CT cholangiography. Eur Radiol. 2007; 17:2531–2537. [PubMed: 17609958]
33. Mehta SR, Thomas EL, Bell JD, Johnston DG, Taylor-Robinson SD. Non-invasive means of measuring hepatic fat content. World J Gastroenterol. 2008; 14:3476–3483. [PubMed: 18567074]

34. Schwenzer NF, Springer-Verlag F, Schraml C, Stefan N, Machann J, Schick F. Non-invasive assessment and quantification of liver steatosis by ultrasound, computed tomography and magnetic resonance. J Hepatol. 2009; 51:433–445. [PubMed: 19604596]

35. Fishbein M, Castro F, Cheruku S, et al. Hepatic MRI for fat quantitation: its relationship to fat morphology, diagnosis, and ultrasound. J Clin Gastroenterol. 2005; 39:619–625. [PubMed: 16000931]

36. Strauss S, Gavish E, Gottlieb P, Katsnelson L. Interobserver and intraobserver variability in the sonographic assessment of fatty liver. AJR. 2007; 189(1449):W320–W323. [web]. [PubMed: 18029843]

Fig. 1.

38-year-old female living potential liver donor with normal serum biochemical results and body mass index. Axial image from CT cholangiogram shows excellent visualization of biliary tract. Bifurcation of right main hepatic duct (*arrow*) is clearly visualized.

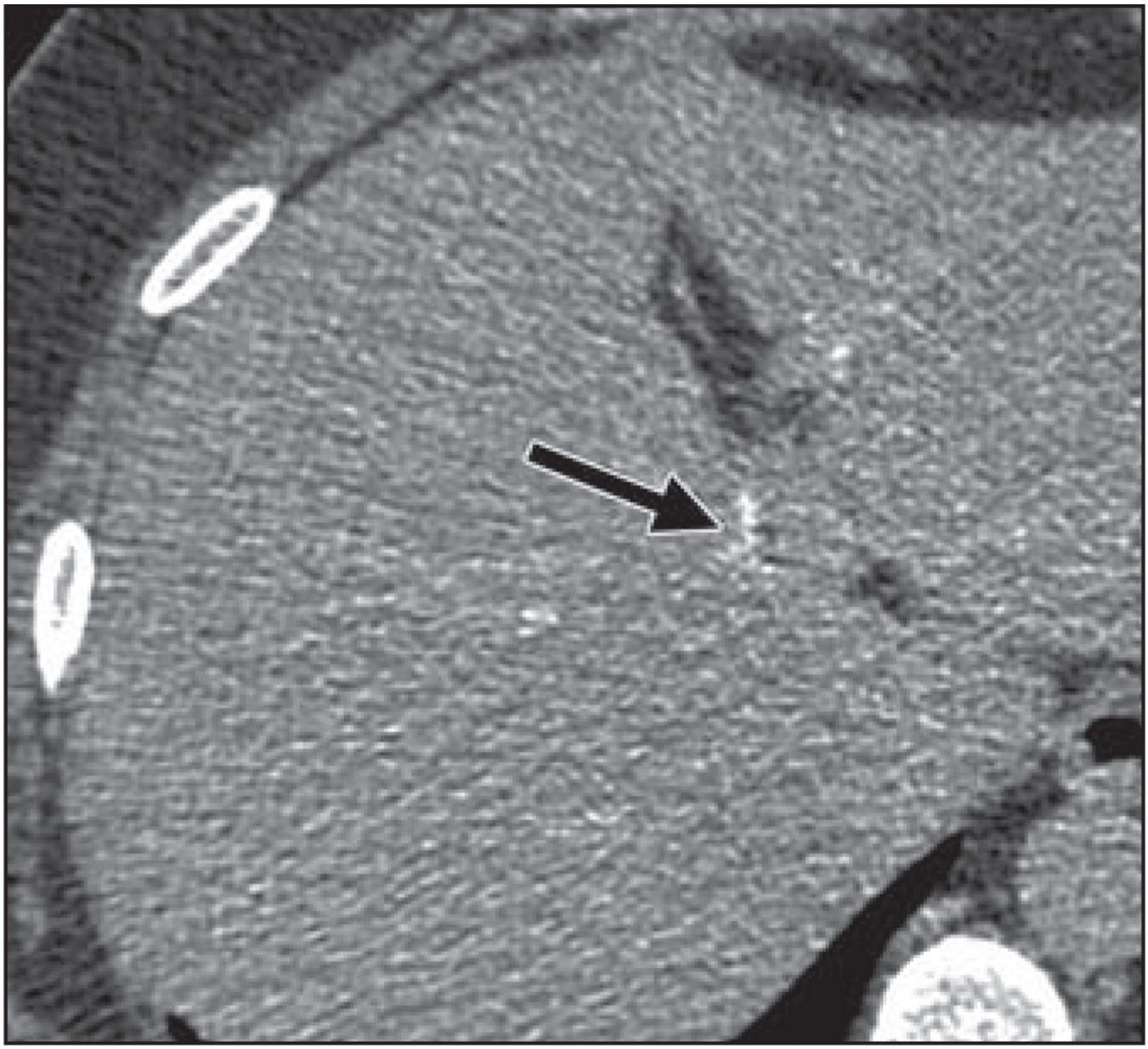

Fig. 2.

47-year-old woman with elevated alkaline phosphatase level of 150 IU/L and body mass index of 31.6. Axial contrast-enhanced CT cholangiogram shows poor visualization of intrahepatic bile ducts. Confluence of right anterior and right posterior (second-order) bile ducts was not clearly seen. Arrow indicates faint visualization of confluence of right and left main ducts.

TABLE 1

Visualization Scores for Biliary Branch Segments

Biliary Branch	Reader 1	Reader 2
Common hepatic duct	2.99 ± 0.08	2.94 ± 0.37
Cystic duct	2.25 ± 1.04	2.37 ± 1.16
First order		
All	2.83 ± 0.41	2.85 ± 0.41
Right main	2.87 ± 0.36	2.84 ± 0.50
Left main	2.82 ± 0.44	2.86 ± 0.40
Second order		
All	2.35 ± 0.66	2.55 ± 0.60
Right anterior	2.50 ± 0.70	2.67 ± 0.65
Right posterior	2.31 ± 0.83	2.60 ± 0.69
Left medial	2.15 ± 0.80	2.27 ± 0.82
Left lateral	2.42 ± 0.79	2.67 ± 0.70
Third order		
All	1.43 ± 0.78	2.53 ± 0.65
Right anterior	1.76 ± 0.92	2.66 ± 0.69
Right posterior	1.45 ± 0.89	2.59 ± 0.79
Left medial	1.04 ± 0.86	2.20 ± 0.93
Left lateral	1.45 ± 0.98	2.66 ± 0.75
All branches	2.15 ± 0.51	2.61 ± 0.50

Note—Data are mean ± SD.

TABLE 2

Values for Serum Tests

Serum Test	Mean (Range)	Normal Reference Range	No. (%) of Patients With Values Above Reference Range (*n* = 130)
Alkaline phosphatase (IU/L)	64.7 (34–150)	34–111	2 (1.5)
Aspartate aminotransferase (IU/L)	24.9 (13–63)	16–41	6 (4.7)
Alanine aminotransferase (IU/L)	27.1 (11–105)	12–59	6 (4.6)
Total bilirubin (mg/dL)	0.9 (0.2–2.3)	0.3–1.3	11 (8.5)
Direct bilirubin (mg/dL)	0.1 (0.1–0.3)	0.1–0.3	0 (0)
Creatinine (mg/dL)	0.9 (0.5–1.4)	0.6–1.2	8 (6.1)[a]

[a] *n* = 117.

TABLE 3

Univariate Analysis: Correlation of Serum Tests and Clinical Findings With Bile Duct Visualization Score

Reader, Parameter	Biliary Branch							
	First Order		Second Order		Third Order		All Biliary Branches	
	r	*p*	*r*	*p*	*r*	*p*	*r*	*p*
Reader 1								
Clinical parameters								
Alkaline phosphatase level	−0.13	0.14	−0.31[a]	>0.001[a]	−0.21[a]	0.02[a]	−0.28[a]	0.002[a]
Aspartate aminotransferase level	−0.08	0.37	−0.10	0.25	−0.02	0.82	−0.06	0.47
Alanine aminotransferase level	−0.15	0.1	−0.16	0.06	−0.11	0.22	−0.16	0.07
Total bilirubin level	−0.11	0.23	−0.04	0.69	−0.07	0.41	−0.05	0.56
Direct bilirubin level	−0.17	0.07	−0.04	0.69	−0.01	0.92	−0.04	0.65
Creatinine level	0.08	0.39	0.07	0.42	−0.02	0.79	0.05	0.59
Body mass index	−0.21[a]	0.03[a]	−0.28[a]	0.003[a]	−0.26[a]	0.007[a]	−0.31[a]	0.001[a]
Age	0.11	0.2	0.04	0.67	0	0.97	0.03	0.74
Imaging parameters								
Patient maximum linear width	−0.19[a]	0.02[a]	−0.22[a]	0.007[a]	−0.21[a]	0.01[a]	−0.25[a]	0.003[a]
CT noise	−0.17[a]	0.04[a]	−0.32[a]	<0.001[a]	−0.38[a]	<0.001[a]	−0.39[a]	<0.001[a]
Ultrasound hepatic steatosis	−0.08	0.38	−0.10	0.23	−0.09	0.3	−0.11	0.19
CT hepatic steatosis	0.1	0.26	0.16	0.06	0.14	0.1	0.15	0.07
Reader 2								
Clinical parameters								
Alkaline phosphatase level	−0.22[a]	0.01[a]	−0.22[a]	0.01[a]	−0.18[a]	0.04[a]	−0.21[a]	0.02[a]
Aspartate aminotransferase level	−0.14	0.13	−0.11	0.2	−0.12	0.17	−0.14	0.11
Alanine aminotransferase level	−0.05	0.54	−0.15	0.09	−0.15	0.08	−0.17	0.06
Total bilirubin level	−0.07	0.46	−0.05	0.57	−0.06	0.48	−0.06	0.49
Direct bilirubin level	−0.07	0.47	0.02	0.83	0.02	0.85	−0.02	0.81
Creatinine level	0.13	0.13	0.08	0.35	0.01	0.87	0.06	0.49
Body mass index	−0.17	0.08	−0.29[a]	0.002[a]	−0.30[a]	0.002[a]	−0.28[a]	0.003[a]

AJR Am J Roentgenol. Author manuscript; available in PMC 2017 February 14.

Reader, Parameter	Biliary Branch							
	First Order		Second Order		Third Order		All Biliary Branches	
	r	*p*	*r*	*p*	*r*	*p*	*r*	*p*
Age	−0.09	0.3	−0.03	0.69	−0.02	0.78	−0.02	0.79
Imaging parameters								
Patient maximum linear width	−0.09	0.27	−0.21[a]	0.01[a]	−0.19[a]	0.02[a]	−0.20[a]	0.02[a]
CT noise	−0.19[a]	0.02[a]	−0.31[a]	<0.001[a]	−0.34[a]	<0.001[a]	−0.32[a]	<0.001[a]
Ultrasound hepatic steatosis	−0.02	0.78	−0.11	0.2	−0.09	0.29	−0.09	0.3
CT hepatic steatosis	0.02	0.81	0.22[a]	0.01[a]	0.27[a]	0.001[a]	0.23[a]	0.005[a]

Note—*r* = Pearson correlation coefficient.

[a] Indicates statistical significance.

TABLE 4

Multivariate Generalized Estimating Equation Results

Parameter	Coefficient	Standard Error	*p*
Alanine aminotransferase level	−0.0009	0.0052	0.85
Alkaline phosphatase level	−0.0082	0.0033	0.01
Body mass index	−0.0291	0.0221	0.19
CT hepatic steatosis	0.0017	0.0062	0.79
Patient maximum linear width	0.0032	0.0031	0.30
CT noise	−0.0141	0.0033	0.02

Note—Wald $\chi^2 = 24.5$ and $p < 0.001$ for the entire model.